



CHORUS

This is the accepted manuscript made available via CHORUS. The article has been published as:

Stabilizing Graphitic Thin Films of Wurtzite Materials by Epitaxial Strain

Dangxin Wu, M. G. Lagally, and Feng Liu

Phys. Rev. Lett. **107**, 236101 — Published 30 November 2011

DOI: [10.1103/PhysRevLett.107.236101](https://doi.org/10.1103/PhysRevLett.107.236101)

Stabilizing Graphitic Thin Films of Wurtzite Materials by Epitaxial Strain

Dangxin Wu,¹ M. G. Lagally,² and Feng Liu^{1,*}

¹*University of Utah, Salt Lake City, Utah 84112*

²*University of Wisconsin, Madison, Wisconsin 53706*

Recent theory [Phys. Rev. Lett. 96, 066102 (2006)] and experiment [Phys. Rev. Lett. 99, 026102 (2007)] show that (0001) ultrathin films of wurtzite (WZ) materials surprisingly transform into a stable graphite-like structure; but the stability is limited to thicknesses of only a few atomic layers. Using first-principles calculations of both freestanding and substrate-supported thin films, we predict that the thickness range of stable graphitic films depends sensitively on strain and can be substantially extended to much thicker films by epitaxial tensile strain. Moreover, the band gap of the stable strained graphitic films can be tuned over a wide range either above or below that of the bulk WZ phase.

PACS numbers: 81.15.Aa,68.35.Bs,64.70.Nd,73.20At

Modern materials growth and synthesis technology has allowed creation of materials that do not exist in nature. Epitaxial growth of thin films, one such technology, creates novel materials by employing two mechanisms: (1) grow thermodynamically metastable thin-film structures by manipulation of growth kinetics, as epitaxial growth conditions are usually far from equilibrium, and (2) convert structures unstable in bulk form into stable thin-film structures by epitaxial strain, which is inherent to heteroepitaxy. One well-known example of the second mechanism is the formation of quantum dots through strain stabilization of three-dimensional islands bounded with otherwise unstable facets[1]. Another appealing example is the recent theoretical prediction[2] that (0001) oriented ultrathin films of WZ materials transform into a new form of stable graphite-like or BN-like structure, subsequently confirmed by an epitaxial-growth experiment[3]. These graphitic films are structurally in analogy with multilayer graphene, which attracted much recent attention, but in a compound form. However, both theory and experiment showed that the stability of the graphitic film is limited to thicknesses of only a few atomic layers.

In this Letter, we predict, using first-principles calculations, that the thickness range of the stability of graphitic films of WZ materials depends strongly on epitaxial strain, and, most importantly, can be greatly extended by applying epitaxial tensile strain. Moreover, the band gap of the stable “strained” graphitic films varies with the strain and film thickness, which can be tuned over a wide range either above or below that of the corresponding bulk WZ material. Our theoretical prediction presents yet another example of epitaxial strain engineering of artificial exotic materials, and provides useful guidelines for future experimental explorations.

Because of their wide and tunable band gaps, WZ materials find a wide range of potential applications. For example, SiC, ZnO, and the III-nitrides, especially GaN, are the most promising candidates for short-wavelength optoelectronic devices, such as light-emitting diodes, laser diodes in high-power, high-temperature microelec-

TABLE I. Maximum number of layers up to which the graphitic structure is stable compared to the WZ structure.

Film	Number of layers (without strain)	Number of layers (5% tensile strain)
InN	8	20
GaN	10	16
ZnO	16	32
AlN	22	48
BeO	28	48
SiC	6	8

tronic devices, and even solar cells[4]. GaN-based violet laser diodes are already used in Blu-rayTM disc technologies and in the Sony[®] PlayStation[®] 3. When doped with transition metals such as Mn, SiC, ZnO, and the III-nitrides are also promising spintronics materials[5]. BeO is a well-known refractory oxide with applications ranging from optoelectronic devices[6] to nuclear reactors[7].

In the WZ structure, alternating hexagonal planes composed of tetrahedral fourfold-coordinated cations and anions are stacked along the c-axis. Cutting the WZ crystals perpendicular to the c-axis to create a (0001) thin film always leads to a cation-terminated surface on one side and an anion-terminated surface on the other side. These are so-called Tasker type III[8] polar surfaces, which are intrinsically unstable due to the divergence of surface energy. Several mechanisms, including vacancy formation, surface reconstruction, and charge transfer from the anion surface to the cation surface, have been proposed for the stabilization of such polar surfaces[9–11]. Most interestingly, recent first-principles calculations[2] predicted that the (0001) thin films of WZ materials (e.g., AlN, BeO, GaN, SiC, ZnO, and ZnS) that are only a few atomic layers thick favor a layered graphitic structure, driven by a new stabilization mechanism for polar surfaces. In the graphitic phase, the cations and anions are arranged in a trigonal-planar coordination, so as to remove the intrinsic surface dipoles and thus to stabilize the film. This prediction was then

confirmed by experiment[3] for ultrathin ZnO films.

In order to take advantage of potential applications of these exotic graphitic forms of WZ materials, it is highly desirable to discover a mechanism to extend the stability of the graphitic phase to a larger range of thicknesses. Here, we propose the idea of applying epitaxial strain to do so. Using first-principles calculations, we examine the stability of both free-standing and substrate-supported thin films in the graphitic structure versus the WZ structure, as a function of strain and film thickness. Our calculations are carried out using the density functional theory method as implemented in the VASP code[12] with the projector augmented wave method[13] and the PBE exchange-correlation functionals[14]. The bulk structures were optimized prior to the film calculations and in all cases the bulk WZ structure is confirmed to be energetically more stable than the bulk graphitic structure. Thin films are modeled by a supercell of a slab with a vacuum layer of at least 15 Å to eliminate spurious interactions between the slabs. Additionally the dipole correction[15] is employed in the calculations of polar surfaces. Convergence tests are done with respect to plane-wave cutoff and k-point sampling. The biaxial epitaxial strain is applied in the basal plane of the thin film and all atomic coordinates are relaxed in the structural optimization. As a further confirmation, a few test calculations were also done using the van der Waals functional[16], which made no difference.

We first compare the relative stability of freestanding graphitic and WZ films as a function of thickness, without applying strain. As pointed out before[2], the comparison of the total energies is the same as the comparison of the cleavage energies. As shown in Table I, our results of the maximum number of layers up to which the graphitic film is more stable than the WZ film for all the materials calculated are in very good agreement with Ref.2. For example, the graphitic GaN thin films are found to be stable up to 10 layers. What this means is that when GaN (0001)/(000 $\bar{1}$) films are equal to or less than 10 layers, the atoms within a bilayer in the WZ structure will relax and converge naturally into a single layer upon structural optimization, forming the graphitic

structure with an ABAB... stacking sequence. Thus, a 10-atomic-layer (0001)/(000 $\bar{1}$) GaN film will transform into a more stable 5 monolayer (ML) graphitic film. In the surface of the graphitic film, there is no destabilizing dipole, as confirmed by the calculated near -zero dipole moments. In contrast, for GaN films beyond 10 layers, the WZ structure tends to be stable. The stabilization of the polar WZ films involves the charge transfer from the (000 $\bar{1}$) bilayer to the (0001) bilayer [2, 10, 11], counteracting the intrinsic dipole perpendicular to the film.

We then proceed to apply biaxial strain on these films. Figure 1(a) shows the total energy as a function of strain, ranging from compressive strain of -5% to tensile strain of 10%, for both WZ and graphitic GaN films of the same thickness. We see that for a 4-layer film, the graphitic phase is more stable than the WZ phase within the whole range of the applied strain. For a 20-layer film, however, the graphitic phase will be more stable only if a biaxial tensile strain larger than 7% is applied; otherwise the WZ phase is more stable. The results of Fig. 1(a) indicate that tensile strain enhances the stability of graphitic films relative to that of WZ films. Further calculations show that increasing tensile strain will increase the thickness range of the stable graphitic phase. For example, with 10% biaxial tensile strain, the graphitic phase of GaN will be stable up to 24 layers. In Table I, we list the maximum number of layers up to which the graphitic films can be stable for each material we considered under 5% applied biaxial tensile strain. Compared to the case without strain, the thickness range for the stable graphitic films is increased significantly by 5% tensile strain, some of them more than doubled.

It is interesting to note that there is a correlation between the ionicity of the compound and the effectiveness of the applied strain. Generally, the more ionic the compound is, the stronger the strain effect will be. Figure 1(b) shows the increased number of stable graphitic layers stabilized by the 5% tensile strain, as a function of the difference of electronegativities ($\Delta\chi$) between the two constituent elements of the compound. Within the group of nitrides or oxides, the effect of strain on enhancing the graphitic film stability increases monotonically as $\Delta\chi$ increases. Relatively speaking, the effect on nitride graphitic films is the strongest; while the effect on SiC, which is more covalent in nature, is the weakest.

Macroscopically, we may understand the tensile strain stabilized graphitic phases in term of the Poisson effect, basically, the biaxial strain stretches the buckled cation-anion bond within the bilayer in the lateral direction while compressing it in the vertical direction (along the c-axis). At the same time the inter-bilayer distance decreases slightly with increasing biaxial tensile strain. Microscopically, we may understand such a strain induced structural transition in terms of an electronic effect, in particular the sp^2 versus sp^3 hybridization energy. We may look at the effect of strain on the energy levels. Fig-

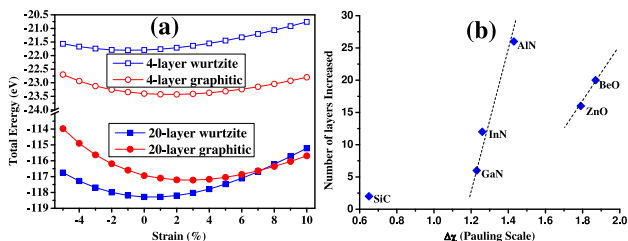


FIG. 1. (color online). (a) The total energy of 4-layer and 20-layer graphitic and WZ GaN films as a function of applied epitaxial strain. (b) The increased number of stable graphitic layers upon applying 5% tensile strain as a function of the difference of Pauling electronegativities ($\Delta\chi$) between the two constituent elements. The dashed lines are for guide of eye.

ure 2 shows the local density of states (DOS) of the O atom in the middle layer of 20-layer ZnO thin films with (5%) and without strain. From our calculation, the 20-layer ZnO WZ film retains the WZ structure without strain, but transforms into a 10 ML graphitic film under 5% tensile strain. In the WZ structure without strain (Fig. 2(a)), the DOS shows that the overlapping O p_x , p_y , and p_z orbitals constitute the valence band maximum, indicative of the tetragonal sp^3 hybridization. As the applied strain increases, we observe a tendency for the p_z orbital to split away from the p_x and p_y orbitals (not shown). When the applied strain is increased to 5%, the p_z orbital is clearly separated from the p_x and p_y orbitals, as seen in the DOS in Fig. 2(b), indicative of the trigonal, planar sp^2 hybridization. In general, there is a close correspondence between the structural transformation and the strain induced energy level splitting and shifting.

We also examined the effect of strain on charge transfer. Through the Bader analysis[17] of atomic charges, we found that strain has a minimal effect on the distribution of atomic charges in either graphitic or WZ films. For the stable graphitic thin films, there is no charge transfer involved in the surface stabilization. The charges on all atoms are very close to the bulk values independent of strain. For the stable WZ thin films, the charge transfer is found highly confined within the two surface layers from anion to cation so as to stabilize the polar surface. But the amount of charge transfer between the two surface layers shows little dependence on the applied strain. Therefore, we conclude that the strain enhanced stability of graphitic films is not caused by any effect of strain on surface-layer charge transfer.

Experimentally, one effective way to strain thin films is by heteroepitaxial growth, in which misfit strain is inherently present due to the lattice mismatch between the growing film and the underlying substrate. To test out this idea, especially to investigate the possible effects of the substrate in addition to strain, we have performed substrate-supported thin-film calculations. As an exam-

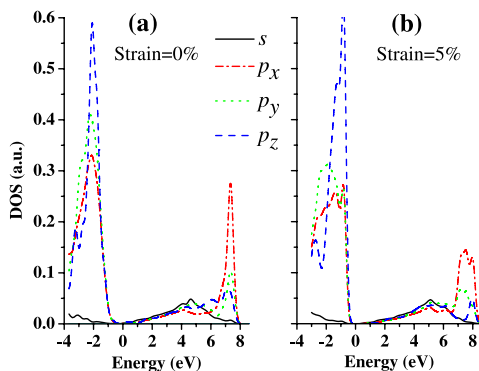


FIG. 2. (color online). Local DOS of the O atoms in the middle layer of a 20-layer ZnO film without (a) and with 5% epitaxial strain (b). Note that after relaxation, the 20-layer WZ film becomes a 10-ML graphitic film at the 5% strain, but remains WZ without strain.

ple, we choose (0001) ZnO films grown on Pb(111), the in-plane lattice constant of Pb (111) plane being about 9% larger than that of the ZnO (0001) plane so that ZnO will be under 9% tensile strain assuming a 1-to-1 lattice matching interface. In the freestanding form, the graphitic ZnO film is found to be stabilized by 9% tensile strain up to 48 layers. On the Pb substrate, the effect of strain stabilization is largely retained assuming a coherence film/substrate interface. Our calculations show that the (0001) ZnO thin film grown on Pb (111) prefers the graphitic structure up to at least 17 MLs over the WZ structure. Figure 3(b) shows that, starting with a WZ structure, a 34-layer ZnO films on a Pb (111) substrate will naturally transform into the more stable 17-ML graphitic structure upon energy minimization.

While a tensile strain increases the thickness up to which graphitic thin films are stable, an applied compressive strain will decrease that thickness. This opposite behavior may help explain some intriguing aspects of the experimental results of graphitic ZnO films grown on Ag (111) substrates[3]. It is interesting to note the experimental observation that the ZnO film is actually under 1.6% of tensile strain, by adopting a 7-to-8 lattice matching interface[3]. If a 1-to-1 interface were adopted, then the ZnO film would be under 10% compressive strain; and if so, the graphitic ZnO film might not have even formed. According to our calculation, under 10% compressive strain, the graphitic phase of ZnO film is unstable for any thickness. As shown in Fig. 3(a), a 3-ML 1-to-1 graphitic ZnO film on Ag (111) substrate is not stable, transforming to the WZ structure after optimization. Experimentally, graphitic ZnO films grown on Ag (111) can only persist up to 2-3 MLs, beyond which they revert back to the WZ phase. This observation was explained as due to possible effects of structural defects and film roughening[3]. Our calculations suggest that relaxation of tensile strain from the 7-to-8 lattice matching as the film grows thicker may also contribute to the desta-

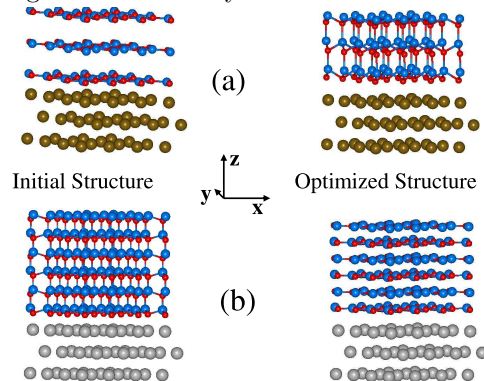


FIG. 3. (color online). (a) The initial and relaxed structures of 6-layer 1-to-1 ZnO film on Ag (111)(3 layers are shown); (b) The initial and relaxed structures of 34-layer ZnO film (only 6 layers are shown) on Pb (111) (3 layers are shown). Zn, O, Ag, and Pb atoms are represented by different ball size and color in ascending order.

bilization of the graphitic phase.

On a related topic, silicene, a single-layer graphitic Si in analogy to graphene, has attracted recent attention[18, 19]. Instead of a planar structure, silicene has been shown to have a low-buckled two-layer structure[19]. We have tried the strain-engineering idea on both freestanding and substrate-supported silicene. No planar structure of silicene can be obtained even under very large strain, although the buckling height is significantly reduced, e.g. from 0.45 Å without strain to 0.29 Å under 20% tensile strain. This result is consistent with our findings above that strain is more effective in stabilizing the graphitic phase of ionic compounds than of covalent compounds like SiC.

All the stable graphitic films are semiconducting, independent of film thickness and applied strain. In contrast, the surfaces of all the stable WZ films are metallic, having non-zero density of states at the Fermi level. It is well known that the band gap of semiconductors depends on the strain[20]. Based on these ideas, a strain-based electronic superlattice has recently been proposed[21]. We found that the band gap of the stable graphitic films varies sensitively with the strain but is less sensitive to film thickness. For example, the band gap of a 2-ML GaN graphitic film will decrease (increase) with increasing tensile (compressive) strain almost linearly, from 2.70 eV with -5% strain to 0.83 eV with 10% strain, as shown in Fig. 4. Although DFT-GGA calculations are well known to underestimate band gaps, as our calculated band gap of 1.75 eV of bulk GaN is much less than the experimental value of 3.51 eV[22], the trend of changing band gap with strain is reliable. So, the calculations suggest that through strain engineering it is possible not only to synthesize stable graphitic films but also to tune their band gaps over a wide range, to be larger or smaller than the band gap of the corresponding bulk WZ phase.

We note that recent calculations[23] suggested that a freestanding (100) film of a BCT ZnO phase could be

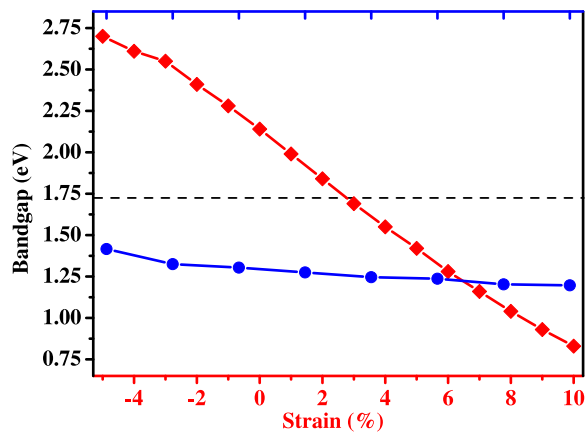


FIG. 4. (color online). Dependence of band gap on the strain for a 2-ML (diamond) graphitic GaN film and on the film thickness for films with 5% tensile strain (circle). The dashed line marks the calculated band gap of bulk GaN.

more stable than the (0001) graphitic film we consider here, in some thickness range. However, those calculations are outside the context of epitaxy we are addressing here. In general, a (100)-oriented BCT film should be much less favored than a (111)- or (0001)-oriented film when epitaxially grown on a (111)- or (0001)-oriented substrate, because of matching of epitaxial symmetry. Furthermore, epitaxial strain is applied in the same manner in the WZ and graphitic film but would have to be different in the BCT film. To confirm this, we have done calculations of BCT films on a Pb substrate, where we found the graphitic film to be most stable (Fig. 3), and as we expected, the BCT films of 6-12 layers, which were found stable in the freestanding form[23], are all unstable in epitaxy, transforming spontaneously into the graphitic phase, as shown in the supplementary information[24]. The results indicate that “epitaxial tensile strain” enhances the stability of graphitic structures relative not only to the the WZ phase but also to the BCT phase.

In conclusion, we have performed first-principles calculations to investigate the possibility of transforming (0001) oriented WZ thin films to the graphitic phase by applying epitaxial (biaxial) strain, for several classes of WZ materials. We demonstrate that the thickness range of stability of the graphitic thin films can be substantially increased by tensile epitaxial strain, but decreased by compressive strain. We further show that as the graphitic thin films are stabilized by strain, their band gap can be tuned over a wide range. The prospect of making single- and multi-layer compound semiconductor films with graphitic structure, in analogy to single- and multi-layer graphene, is very appealing, with broad implications in both fundamental research and technology applications. We await future experiments to confirm our theoretical predictions.

This work is supported by DOE-BES (Grant No. DE-FG02-03ER46027;-03ER46028). The calculations were carried out using computing facilities at NERSC and CHPC of the University of Utah. The authors thank C. Freeman, J. Harding and B. J. Morgan for helpful discussions. The crystal structures in Fig. 3 were plotted by using VESTA software[25].

* fliu@eng.utah.edu

- [1] G.H. Lu and F. Liu, Phys. Rev. Lett. **94**, 176103 (2005); G.H. Lu, M. Cuma, and F. Liu, Phys. Rev. B **72**, 125415 (2005).
- [2] C. L. Freeman, F. Claeysens, N. L. Allan, and J. H. Harding, Phys. Rev. Lett. **96**, 066102 (2006).
- [3] C. Tusche, H. L. Meyerheim, and J. Kirschner, Phys. Rev. Lett. **99**, 026102 (2007).
- [4] R. Dahal et al., Appl. Phys. Lett. **97**, 073115 (2010).
- [5] A. J. Bauer et al., Materials Science Forum, **645-648**, 395 (2010).

- [6] V. Ivanov et al., *Radiat. Meas.* **42**, 742 (2007).
- [7] P.I.F.Zhezherun et al., *At. Energy* **13**, 860 (1963).
- [8] P. W. Tasker, *J. Phys. C* **12**, 4977 (1979).
- [9] C. Noguera, *J. Phys. Condens. Matter* **12**, R367 (2000).
- [10] A. Wander et al., *Phys. Rev. Lett.* **86**, 3811 (2001).
- [11] J. M. Carlsson, *Comput. Mater. Sci.* **22**, 24 (2001).
- [12] G. Kresse, and J. Hafner, *Phys. Rev. B* **47**, 558 (1993).
- [13] P. E. Blöchl, *Phys. Rev. B* **50**, 17953 (1994); G. Kresse, and J. Joubert, *Phys. Rev. B* **59**, 1758 (1994).
- [14] J. P. Perdew, K. Burke, and M. Ernzerhof, *Phys. Rev. Lett.* **77**, 3865 (1996).
- [15] J. Neugebauer and M. Scheffler, *Phys. Rev. B* **46**, 16067 (1992); G. Makov and M. C. Payne, *Phys. Rev. B* **51**, 4014 (1995).
- [16] K. Lee, E. D. Murray, L. Kong, B. I. Lundqvist, and D. C. Langreth, *Phys. Rev. B*, **82**, 081101(R) (2010); L. Kong, private communication.
- [17] G. Henkelman, A. Arnaldsson, and H. Jonsson, *Comput. Mater. Sci.* **36**, 354 (2006).
- [18] G. Guzmán-Verri and L. C. Lew Yan Voon, *Phys. Rev. B* **76**, 075131 (2007).
- [19] S. Cahangirov, et al., *Phys. Rev. Lett.* **102**, 236804 (2009).
- [20] G. H. Olsen, C. J. Nuese, and R. T. Smith, *J. Appl. Phys.* **49**, 5523 (1978).
- [21] Z. Liu et al., *Phys. Rev. Lett.* **105**, 016802 (2010).
- [22] I. Vurgaftman and J. R. Meyer, *J. Appl. Phys.* **94**, 3675 (2003).
- [23] J. Wang et al., *Phys. Rev. B* **76**, 172103 (2007); B. J. Morgan, *Phys. Rev. B* **80**, 174105 (2009); B. J. Morgan, *Phys. Rev. B* **82**, 153408 (2010).
- [24] See Supplementary Material at (url) for the comparison of the relative stability of BCT and graphitic films on a Pb (111) substrate.
- [25] K. Momma and F. Izumi, *J. Appl. Crystallogr.* **41**, 653 (2008).